Orientation of the Saccharide Chains of Glycolipids at the Membrane Surface: Conformational Analysis of the Glucose–Ceramide and the Glucose–Glyceride Linkages Using Molecular Mechanics (MM3)†

Per-Georg Nyholm* and Irmin Pascher

Structural Chemistry, Department of Medical Biochemistry and MEDNET Laboratory, University of Göteborg, Medicinaregatan 9, 413 90 Göteborg, Sweden

Received April 16, 1992; Revised Manuscript Received October 28, 1992

ABSTRACT: Preferred conformations of the saccharide–ceramide linkage of glucosylceramides with different ceramide structures (normal and hydroxy fatty acids) were investigated by molecular mechanics (MM3) calculations and compared with conformational features obtained for glucosylglycerolipids (diacyl and dialkyl analogues). Relaxed energy map calculations with MM3 were performed for the three bonds (C1′–O1–C1–C2, torsion angles ϕ, ψ, and θ_1) of the glucose–ceramide/diglyceride linkage at different values of the dielectric constant. For the ϕ torsion of the glycosidic C1′–O1 bond the calculations show a strict preference for the +sc range whereas the ψ/θ_1 energy surface is dependent on the structure of the lipid moiety as well as on the dielectric constant (ϵ). Calculations performed on glucosylceramide with normal and hydroxy fatty acids at $\epsilon = 4$ (bilayer subsurface conditions) show three dominating conformers (ψ/θ_1 = ap/–sc, –sc/ap, and ap/ap). The ap/–sc conformer, which represents the global energy minimum, is stabilized by polar interactions involving the amide group. The +sc rotamer of θ_1 is unfavored in sphingolipids due to a Hassel–Ottar effect involving the sphingosine O3 and O1 oxygen atoms. Comparative calculations on glycosylglycerolipid analogues (ester and ether derivatives) show a distinct preference for the ap rotamer of θ_1. An evaluation of the steric hindrance imposed by the surrounding membrane surface shows that in a bilayer arrangement the range of possible conformations for the saccharide–lipid linkage is considerably reduced. The significance of preferred conformations of the saccharide–ceramide linkage for the presentation and recognition of the saccharide chains of glycosphingolipids at the membrane surface is discussed.

There is increasing evidence that carbohydrates attached to lipids or membrane proteins are involved in a variety of recognition processes at the cell surface. Especially glycosphingolipids (GSLs)[1] have received much attention due to their role as blood group, transplantation, and tumor antigens (Hakomori, 1989, 1990) and as receptors for bacteria and viruses (Karlsson, 1989). Recent conformational studies of glycosphingolipids with blood group A activity (Nyholm et al., 1989) and receptor activity for uropathogenic *Escherichia coli* bacteria (Strömberg et al., 1991) suggest that the orientation and steric presentation of the saccharide chain at the membrane surface are of importance for the recognition of GSLs by antibodies and bacterial adhesins. Furthermore, these studies indicate that the orientation of the saccharide head group is primarily determined by the conformation of the linkage between the saccharide head group and the ceramide moiety (torsion angles ϕ, ψ, θ_1 in Figure 1).

Experimental data of relevance for the saccharide–ceramide linkage are available from X-ray crystal analyses on cerebrosides (Pascher & Sundell, 1977; Nyholm et al., 1990) and NMR studies of glucosylceramide (Skarjune & Oldfield, 1982) and glucosylglyceride (Jarrell et al., 1987). These experimental data, however, show some differences with respect to the orientation of the saccharide head group. Theoretical calculations of preferred conformations performed

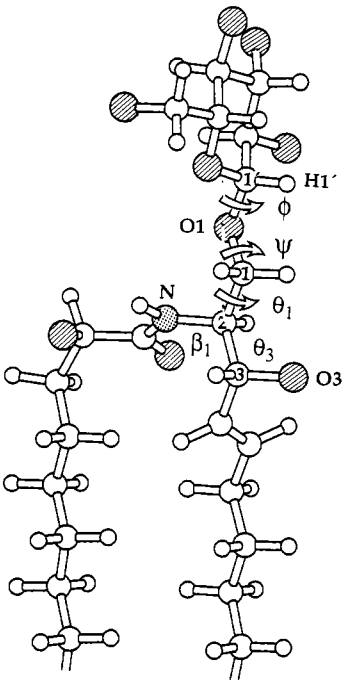

FIGURE 1: Atom numbering and notation of torsion angles. The conformation of the saccharide–lipid linkage is determined by the three torsion angles, ϕ, ψ, and θ_1, which are defined as follows: ϕ, H1′–C1′–O1–C1; ψ, C1′–O1–C1–C2; θ_1, O1–C1–C2–C3. The molecule shown in the figure is GlcCer(h) with truncated chains. The conformation of the glucose–ceramide linkage in this case is $\phi/\psi/\theta_1$ = 42°/180°/180° (cf. conformer 5, Figure 3b).

† This work is supported by the Swedish Medical Research Council (Grant 006), the Alice and Knut Wallenberg Foundation, and the Skandinaviska Enskilda Bank Foundation. A preliminary report on this work was presented at the 11th International Symposium on Glycoconjugates, Toronto, Canada, 1991. This research is part of a dissertation submitted by P.-G.N. in fulfillment of the requirements for the Ph.D degree from the University of Göteborg.

[1] Abbreviations: GSLs, glycosphingolipids; GlcCer(n) and GlcCer(h), glucosylceramide with normal (n) and 2-hydroxy (h) fatty acid; GlcDAG, glucosyldiacylglycerol; GlcDEG, glucosyldialkylglycerol; NMR, nuclear magnetic resonance.

0006-2960/93/0432-1225$04.00/0

for galactosyl- and glucosylceramides (Wynn et al., 1986; Nyholm et al., 1989, 1990) also indicate several favored conformations for the saccharide–ceramide linkage.

In the present study, molecular mechanics MM3 (Allinger et al., 1989) was applied in order to obtain a detailed description of the conformational space for the saccharide–ceramide linkage. The calculations were performed on β-D-glucosylceramide (GlcCer), which is by far the most abundant basic structure in GSLs (Kanfer & Hakomori, 1983). Diacyl- and dialkylglucosylglycerolipids were included in the investigation in order to explore possible conformational differences between sphingolipids and glycerolipids. Special attention was paid to the significance of intramolecular hydrogen bonds and dipole–dipole interactions. Furthermore, the steric restrictions imposed by the surrounding membrane surface on the conformation of the saccharide head group were investigated.

METHODS

Modeling Software. Preliminary calculations were performed using the GESA program (Paulsen et al., 1984) and molecular mechanics MM2(87) (Allinger, 1977; Lii et al., 1989). The results presented in this paper were, however, predominantly obtained by calculations with MM3 (1990 version; Allinger et al., 1989; Lii & Allinger, 1991). In the MM3 force field the electrostatic energy of a noncharged polar molecule is calculated from dipole–dipole interactions. Bond dipoles from the standard parameter list of MM3 were used throughout this study. The hydrogen bond energy in MM3 is mainly accounted for by dipole–dipole interactions and to a lesser extent by the VDW interaction term, using special VDW parameters for atoms able to form hydrogen bonds (Lii & Allinger, 1991). The exo-anomeric effect is accounted for by dipole–dipole interactions, and corrections are made for changes in bond length of the C–O bonds at the anomeric carbon (Norskov-Lauritsen & Allinger, 1984; Allinger et al., 1990). The MM3 force field offers significant improvements as compared to MM2(87), e.g., with respect to the parametrization of hydrogen bonds, and has been successfully applied for calculations on saccharides (French et al., 1990a; Dowd et al., 1992).

In addition, comparative calculations were performed with MOPAC, version 5 (Stewart, 1990)[2] using AM1 (Dewar et al., 1985). All calculations were carried out on a Convex C120 computer.

For structure manipulation and graphical display the Chem-X program (Chemical Design Ltd., Oxford, England) running on a VAXcluster (μVAX 3400 and a VAXstation 3200) was used.

Contour maps and grid maps for the visualization of energy and probability data were generated with the UNIMAP program (UNIRAS A/S, Søborg, Denmark).

Modeling of Starting Conformations of Glucosylceramides and Glucosylglycerides. The following five glycolipid model compounds were studied: (**1**) GlcCer(n), β-D-glucosylceramide containing 4-sphingenine and normal fatty acid; (**2**) GlcCer(h), the corresponding β-D-glucosylceramide with 2-D-hydroxy fatty acid; (**3**) GlcCer(NCH_3), the N-methylated derivative of compound **1**; (**4**) GlcDAG, β-D-glucosyldiacylglycerol (ester analogue); (**5**) GlcDEG, β-D-glucosyldialkylglycerol (ether analogue). The atom numbering and notation of torsion angles for these compounds is shown in Figure 1. For the description of staggered and eclipsed torsion angle ranges the notation of Klyne and Prelog (1960) is used.

GlcCer(n) was modeled starting from the crystal structure of β-glucose (Chu & Jeffrey, 1968) and from the ceramide moiety of cerebroside crystal structures (Pascher & Sundell, 1977; Nyholm et al., 1990). The bent and tilted hydrocarbon chains observed in the cerebroside crystal structures were straightened by adjustment of a few torsion angles to resemble the hydrocarbon chain conformations predominantly observed for membrane lipids (Hauser et al., 1981; Pascher et al., 1992). Furthermore, the sphingosine and fatty acid chains were truncated at atoms C6 and C5, respectively, in order to reduce the computing time for the calculations of energy maps (see below).

The model structure of GlcCer(n) was then subjected to full energy minimization with MM3 at a dielectric constant of $\epsilon = 4$. With respect to the torsion angles (β_1, β_2, β_3, and θ_3) of the polar ceramide part, this minimized conformation showed only minor differences as compared to the corresponding torsion angles found in the crystal structure of cerebroside.

From this energy-minimized conformation of GlcCer(n) the geometries of the other glycolipid model compounds, GlcCer(h), GlcCer(NCH_3), GlcDAG, and GlcDEG, were generated by substitution of specific functional groups using the Chem-X program followed by energy minimization with MM3.

In order to account for different rotamers of the glucose 6-hydroxymethyl group both the *gg* and the *gt* conformers [for definition see Jeffrey (1990)] of GlcCer(n) and GlcCer(h) were tested. These calculations gave very similar results for the *gg* and *gt* conformers. Since NMR studies have shown that the *gg* conformer is dominating in GlcCer (Poppe et al., 1990) and GlcDEG structures (Jarrell et al., 1986; Renou et al., 1989), this conformer was used in all further calculations. Furthermore, the secondary hydroxyl groups of the glucose residue were arranged in an anticlockwise (*R*) orientation (Ha et al., 1988). This is in agreement with our preliminary MM3 calculations on β-methoxyglucose, which showed that the *R* orientation is energetically more favorable than the clockwise *C* orientation of the hydroxyl groups.

As a precaution for the following map calculations the torsion angles ψ and θ_1 were adjusted to $\psi/\theta_1 = 180°/180°$ corresponding to an energy minimum with a fully extended conformation of the saccharide–ceramide linkage (Nyholm et al., 1990). Hereby the bias due to the use of crystal structures as starting conformations was avoided.

After complete minimization with MM3 at a dielectric constant of 4, the obtained geometries for model structures **1–5** were used as starting conformations for the energy map calculations.

Calculation of Conformational Energy Maps and Probability Maps. The conformational energy as a function of the torsion angles of the saccharide–ceramide linkage (see Figure 1) was calculated with MM3 in the form of two-dimensional ϕ/ψ and ψ/θ_1 maps. These maps were generated as relaxed energy maps; i.e., energy minimization was performed at each grid point. The minimization included all degrees of freedom except for the torsion angles defining the respective grid point (cf. MM3 driver option −1). In order to avoid the problem of inelastic deformations (French, 1988) during the driver calculation, the DRIVER subroutine was modified to generate the starting geometry at each grid point by rigid rotation of the initially modeled starting conformation

[2] The MOPAC program is available at QCPE, order no. 455. For the present calculations MOPAC version 5 (1989) in vectorized form was acquired through Convex Inc. (Richardson, TX).

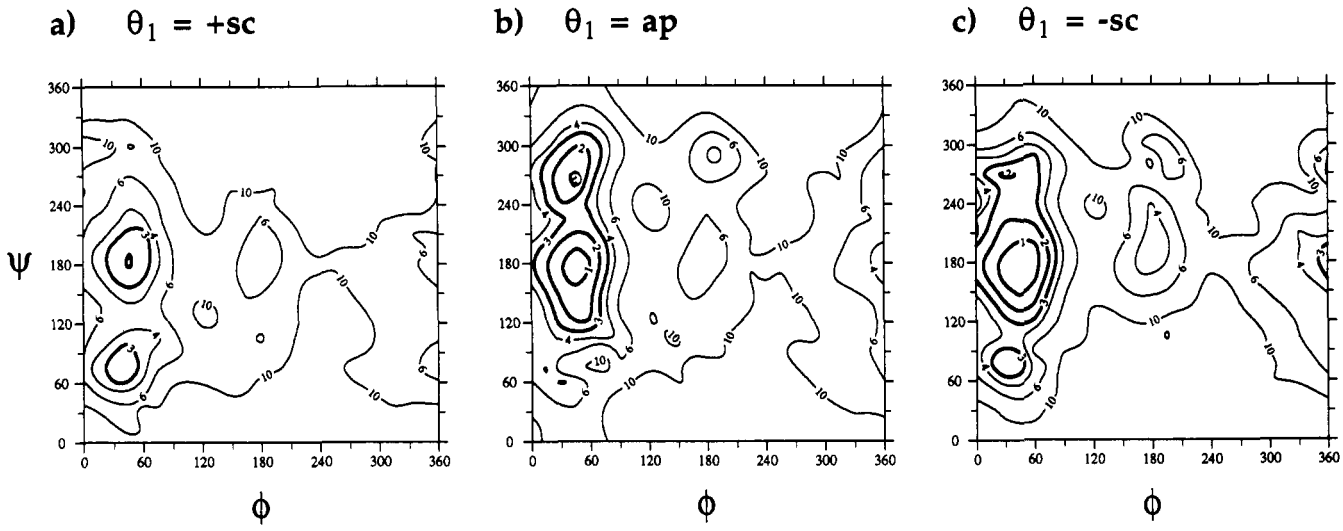

FIGURE 2: Relaxed ϕ/ψ energy maps of GlcCer(n) calculated with MM3 with a dielectric constant of 4. The calculations were performed for the three staggered conformations of θ_1: +sc (a), ap (b), and –sc (c) (initial geometry: $\theta_1 = 60°$, 180°, and –60°, respectively). The contour lines of the energy maps (a–c) refer to the conformational energy (kcal/mol) in relation to the lowest minimum which is found in the ϕ/ψ map at θ_1 = –sc (c, $\phi/\psi = 45°/180°$). From the ϕ/ψ maps (a–c) it is apparent that the favored conformations for ϕ are confined to a limited range of +sc whereas the torsion angle ψ shows a rather wide low-energy range.

(French et al., 1990b). The step size for the relaxed energy map calculations was 15°.

In order to evaluate the significance of intramolecular electrostatic interactions, the energy map calculations were carried out at three different values of the dielectric constant: $\epsilon = 80$, $\epsilon = 4$, and $\epsilon = 1.5$. At $\epsilon = 80$ the electrostatic interactions are highly attenuated, corresponding to conditions in bulk water. An ϵ value of 4 allows significant hydrogen bonds and dipole–dipole interactions and is often used for molecular mechanics calculations on crystal structures of small molecules and of proteins (Lii et al., 1989). In the present calculations $\epsilon = 4$ was used to account for the dielectric properties of a lipid bilayer at the level of the saccharide–ceramide linkage, i.e., at the interface between the hydrocarbon matrix and the head-group region (see Discussion). Calculations at an ϵ value of 1.5, which corresponds to in vacuo conditions, were performed to emphasize the polar interactions allowing a more efficient sampling of possible intramolecular hydrogen bonds and dipole–dipole interactions.

On the basis of ϕ/ψ and ψ/θ_1 energy maps calculated with MM3, weight factors and probabilities for the different conformers were calculated assuming a Boltzmann distribution at 310 K (Cumming & Carver, 1987).

Final Energy Minimization. Selected conformations (**1–9**, Figure 3a) of the ψ/θ_1 energy maps obtained at different ϵ values were subjected to further energy minimizations which also included the ψ and θ_1 torsion angles. Furthermore, the final geometries obtained for GlcCer(n) by the MM3 calculations at $\epsilon = 1.5$ were used as input for comparative calculations with MOPAC using AM1 and the keywords MMOK, GNORM = 1.0, and XYZ.

Conformational Restrictions Imposed by the Membrane Layer. In order to evaluate the steric interference of the head group with the surrounding membrane surface, a restriction plane was introduced at the level of the sphingosine atom C1 and perpendicular to the C1···C3 axis (Nyholm et al., 1989). The minimum distances between this restriction plane and the atoms of the glucose head group were calculated as a function of ψ and θ_1 and plotted as contours in a ψ/θ_1 map. In this calculation rigid geometry was assumed for the glucose residue and for the ϕ torsion angle ($\phi = 42°$).

RESULTS

ϕ/ψ Energy Maps. Figure 2 shows the ϕ/ψ energy maps of GlcCer(n) obtained with MM3 with $\epsilon = 4$ at the three staggered conformations (+sc, ap, and –sc) of θ_1. As apparent from Figure 2 the torsion angle ϕ shows a distinct preference for the +sc range. This preference of ϕ is not significantly affected by changes of the torsion angles ψ and θ_1 (Figure 2) nor by changes in the dielectric constant or by the described modifications of the ceramide/diglyceride moiety.

In view of the constancy of the ϕ torsion angle the calculations were focused on the exploration of the ψ/θ_1 potential energy surface which shows more complex features.

ψ/θ_1 Energy Maps of GlcCer(n). Figure 3a shows the characteristic features of the relaxed ψ/θ_1 energy map of GlcCer(n) derived from MM3 calculations with a dielectric constant of 80. This ψ/θ_1 map shows rather extensive low-energy surfaces comprising the staggered conformations of θ_1 and a rather wide range for the torsion angle ψ ($180 \pm 100°$). In order to facilitate the discussion of different ψ/θ_1 conformations, the low-energy surface of the ψ/θ_1 map was divided into nine basic regions which were marked with the numerals 1–9 (Figure 3a). Conformations representative for these nine regions are shown in Figure 3b.

At $\epsilon = 80$, corresponding to conditions with highly attenuated electrostatic interactions, the ψ/θ_1 energy map (Figure 3a and Table I) shows its lowest energy minimum at ψ/θ_1 = ap/ap (conformer 5), followed by minima at ψ/θ_1 = ap/–sc (conformer 2), ψ/θ_1 = –sc/ap (conformer 6), and ψ/θ_1 = ap/+sc (conformer 8). The results of the final energy minimizations are given in Table I. The calculated population distribution is shown in the combined energy/probability ψ/θ_1 map (Figure 3c and Table I). The distribution on the three staggered rotamers of θ_1 = +sc:ap:–sc is 11:55:33% (Table II).

If intramolecular interactions are accounted for by using lower values of the dielectric constant ($\epsilon = 4$ and 1.5), the features of the relaxed ψ/θ_1 energy/probability maps are profoundly altered (Figure 3d,e).

For $\epsilon = 4$ (Figure 3d and Table I) the –sc rotamer of θ_1 becomes favored, resulting in a population distribution of the θ_1 rotamers +sc:ap:–sc of 4:47:48% (Table II) and a domi-

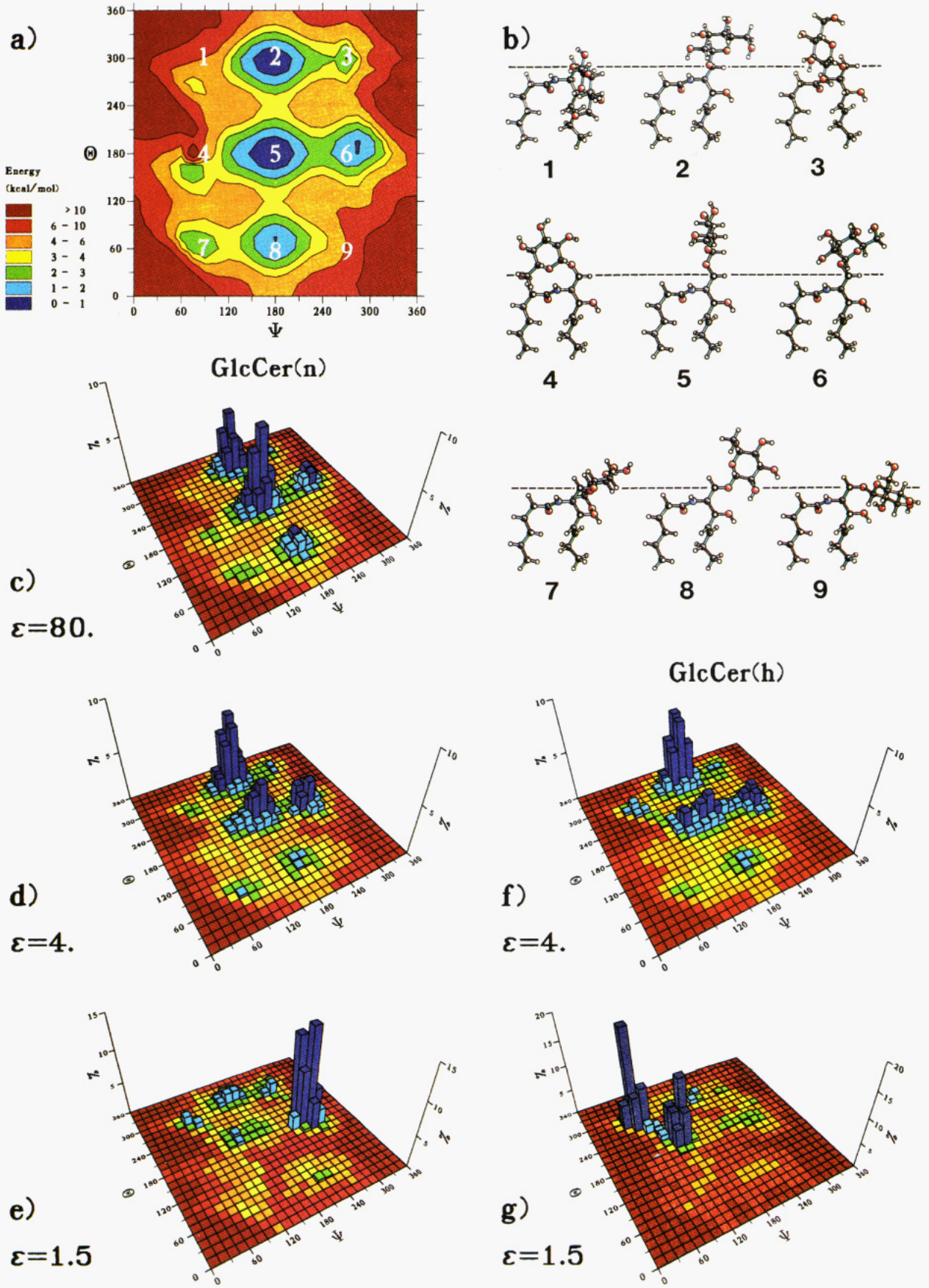

FIGURE 3: (a) Relaxed ψ/θ_1 energy map for GlcCer(n) calculated with MM3 at a dielectric constant of 80. Nine conformational regions of the ψ/θ_1 energy map have been indicated by numerals 1–9 (see text for discussion). (b) Ball-and-stick models of GlcCer(n) with ψ/θ_1 conformations corresponding to the positions of the labels in panel a. The conformations shown are the starting geometries for calculations at the indicated points (ψ = 90°, 180°, –90°; θ_1 = 60°, 180°, –60°). (c–g) Combined energy and probability ψ/θ_1 maps for GlcCer based on MM3 relaxed map calculations. The energy is shown by the color coding whereas the probabilities according to a Boltzmann distribution are shown by the height of the bars. For GlcCer(n) the results from calculations at three different values of the dielectric constant, ϵ = 80 (c), ϵ = 4 (d), and ϵ = 1.5 (e), are shown. The corresponding energy/probability maps for GlcCer(h) at ϵ = 4 (f) and ϵ = 1.5 (g) are shown for comparison.

Table I: Minimum Energy Conformations and Conformer Populations for Compounds **1**, **2**, **4**, and **5**[a]

conf no.	ϕ (deg)	ψ (deg)	θ_1 (deg)	β_1 (deg)	ΔE[b] (kcal/mol)	population[c] (%)
			GlcCer(n), MM3, ϵ = 80			
2	45	178	−63	142	0.10	32
3	45	−124	−62	139	2.66	1
4	24	76	160	144	2.22	1
5	43	179	179	143	0 (E_0 = 26.69)	46
6	42	−82	−178	140	0.86	10
7	46	98	72	137	2.73	1
8	47	−178	71	140	0.79	10
			GlcCer(n), MM3, ϵ = 4			
1	34	77	−93	138	2.12	1
2*	47	178	−64	141	0 (E_0 = 23.27)	46
3	32	−96	−61	82	1.48	2
5*	43	179	−179	145	0.50	28
6*	45	−90	167	96	0.65	19
7	42	76	61	81	2.06	1
8*	45	176	69	135	1.73	3
			GlcCer(n), MM3, ϵ = 1.5			
1	33	77	−93	137	1.30	4
2	42	166	−73	140	1.24	13
3	38	−110	−77	132	0.45[Δ]	6
4/5	50	134	−167	153	1.59	4
5	46	180	−166	150	2.09	3
6	46	−90	166	95	0 (E_0 = 14.65)	68
8/9	37	−156	61	82	1.02[Δ]	1
			GlcCer(n), MOPAC, AM1[d]			
1	31	84	−95	114	1.22	
2	36	173	−76	115	2.07	
3	28	−99	−78	119	1.17	
4/5	50	128	−178	126	2.06	
5	50	−170	175	118	2.07	
6	40	−89	161	103	0 (E_0 = −407.30)	
8	37	−163	65	110	2.05	
			GlcCer(h), MM3, ϵ = 80			
2	45	178	−62	132	0.18	32
3	42	−108	−60	105	2.21	1
5	44	180	179	132	0 (E_0 = 28.62)	46
6	43	−75	180	127	0.93	10
7	42	78	62	120	2.15	1
8	43	180	75	132	0.99	9
			GlcCer(h), MM3, ϵ = 4			
1	34	75	−94	136	1.17	2
2	47	179	−63	125	0 (E_0 = 22.44)	48
3	38	−106	−61	108	1.94	2
4/5	48	135	−179	137	0.84	8
5	45	180	180	132	0.65	22
6	44	−91	179	107	0.79	13
7	41	77	60	91	2.46	<1
8	47	−177	71	114	1.66	3
			GlcCer(h), MM3, ϵ = 1.5			
1*	37	76	−94	142	0 (E_0 = 7.92)	45
2	37	−164	−79	96	1.42	5
4/5*	52	130	−167	143	0.23	44
6	46	−92	178	104	2.25	5
			GlcDAG, MM3, ϵ = 4			
2	45	180	−56	132	0.39	19
5	50	−180	179	132	0 (E_0 = 19.32)	41
6	42	−89	168	106	0.22	21
7	44	78	60	131	0.54	12
8	44	172	64	131	1.34	5
			GlcDEG, MM3, ϵ = 4			
2	43	180	−57	165	0.05	35
4	33	73	153	166	1.47	3
5	49	179	177	163	0 (E_0 = 28.06)	40
6	46	−77	−180	162	1.02	7
7	39	79	60	159	1.82	2
8	49	−178	70	162	0.77	12

[a] The table shows the torsion angles ϕ, ψ, and θ_1 (in degrees) for selected minimum energy conformations of the model compounds **1**, **2**, **4**, and **5** obtained after complete MM3 minimization (including ψ and θ_1) at different values of the dielectric constant. The conformations are labeled according to their location in the different regions of the ψ/θ_1 diagram (see Figure 3a). Conformations indicated by an asterisk are shown in Figure 5. [b] The ΔE column contains the final steric energy relative to the conformation with the lowest energy at the applied ϵ value. The absolute value of the lowest final steric energy is given in parentheses. Energy minima indicated by (Δ) are narrow minima in the ψ/θ_1 map which were not registered in the relaxed map calculation with step size 15°. [c] The populations of the different conformers were integrated from the peaks of the ψ/θ_1 maps (cf. Figures 3c–g and 4a–c). [d] In the results of single point minimizations with MOPAC (AM1) on GlcCer(n), the ΔE values are based on the final heat of formation.

Table II: Calculated Population Distribution (%) for Rotamers of θ_1[a]

		$\epsilon = 80$	$\epsilon = 4$	$\epsilon = 1.5$
GlcCer(n)	+sc	11	4	1
	ap	55	47	75
	−sc	33	48	23*
GlcCer(h)	+sc	10	4	0
	ap	56	44	49
	−sc	34	52	51*
GlcCer(NCH_3)	+sc	13	10	3
	ap	78	79	95
	−sc	8	10	1
GlcDAG	+sc	9	17	36
	ap	69	63	61
	−sc	22	20	1
GlcDEG	+sc	9	13	18
	ap	61	49	29
	−sc	29	37	51

[a] Calculated population distribution for rotamers of θ_1 for compounds **1**–**5** at different dielectric constants. Values marked with an asterisk include population peaks which are not fully located within the given staggered range (±30°) (cf. Table I). The data are integrated values from the ψ/θ_1 probability maps.

nating energy minimum for conformer 2 ($\psi/\theta_1 = 178°/-64°$; see Table I). The –sc conformation of θ_1 is stabilized by interactions between the antiparallel C1–O1 and the N–H bond dipoles and by a hydrogen bond contact between the N–H hydrogen and the glycosidic oxygen O1 (cf. Figure 5a).

In the corresponding ψ/θ_1 map calculated with $\epsilon = 1.5$ (Figure 3e) the dominating energy minimum is located at $\psi/\theta_1 = -90°/167°$ (conformer 6, Table I). This conformation is stabilized by a hydrogen bond between the 2-hydroxyl group of the glucose residue and the fatty acid carbonyl oxygen atom (cf. Figure 5c). The results of these MM3 calculations at $\epsilon = 1.5$ are in good agreement with comparative MOPAC calculations (Table I).

A notable feature common to the three ψ/θ_1 energy and probability maps of GlcCer(n) derived at different ϵ values (Figure 3c,d,e) is that the conformational range of θ_1 = +sc is distinctly disfavored (see also Table II).

ψ/θ_1 Energy Maps of GlcCer(h). The relaxed ψ/θ_1 energy and probability maps for GlcCer(h) obtained by MM3 calculations at $\epsilon = 80$ (not shown) and $\epsilon = 4$ (Figure 3f) show a close similarity with the corresponding maps of GlcCer(n) (Figure 3c,d). The +sc rotamer of θ_1 in GlcCer(h) is unfavored as in the case of GlcCer(n) (Table II). The torsion angles of the major minimum energy conformations of GlcCer(h) (conformer 2, 5, and 6, Table I) are in agreement with those obtained for GlcCer(n).

However, the calculations carried out on GlcCer(h) with $\epsilon = 1.5$ (Figure 3g) show two energy minima, at $\psi/\theta_1 = 75°/-94°$ (conformer 1, Figure 5e and Table I) and $\psi/\theta_1 = 135°/-179°$ (conformer 4, Figure 5f and Table I), which were not observed in the corresponding ψ/θ_1 map of GlcCer(n) (Figure 3e). In both these conformers the 2-OH group of the fatty acid is involved in a hydrogen bond to the 6-hydroxyl group of the glucose residue. Furthermore, conformers 1 and 4 of GlcCer(h) are stabilized by a hydrogen bond between the amide nitrogen and the O5 ring oxygen of the glucose residue.

It should be noted that conformers 1 and 4, which dominate in calculations at $\epsilon = 1.5$ (Figure 3g), do not persist as dominating conformations if the ψ/θ_1 energy map is recalculated at $\epsilon = 4$ (Figure 3f) starting from coordinates obtained at $\epsilon = 1.5$.

ψ/θ_1 Energy Maps of GlcCer(NCH_3). Comparative calculations on GlcCer(NCH_3) (Figure 4a, Table II) show that the –sc rotamer of θ_1 is less favorable than in the case of

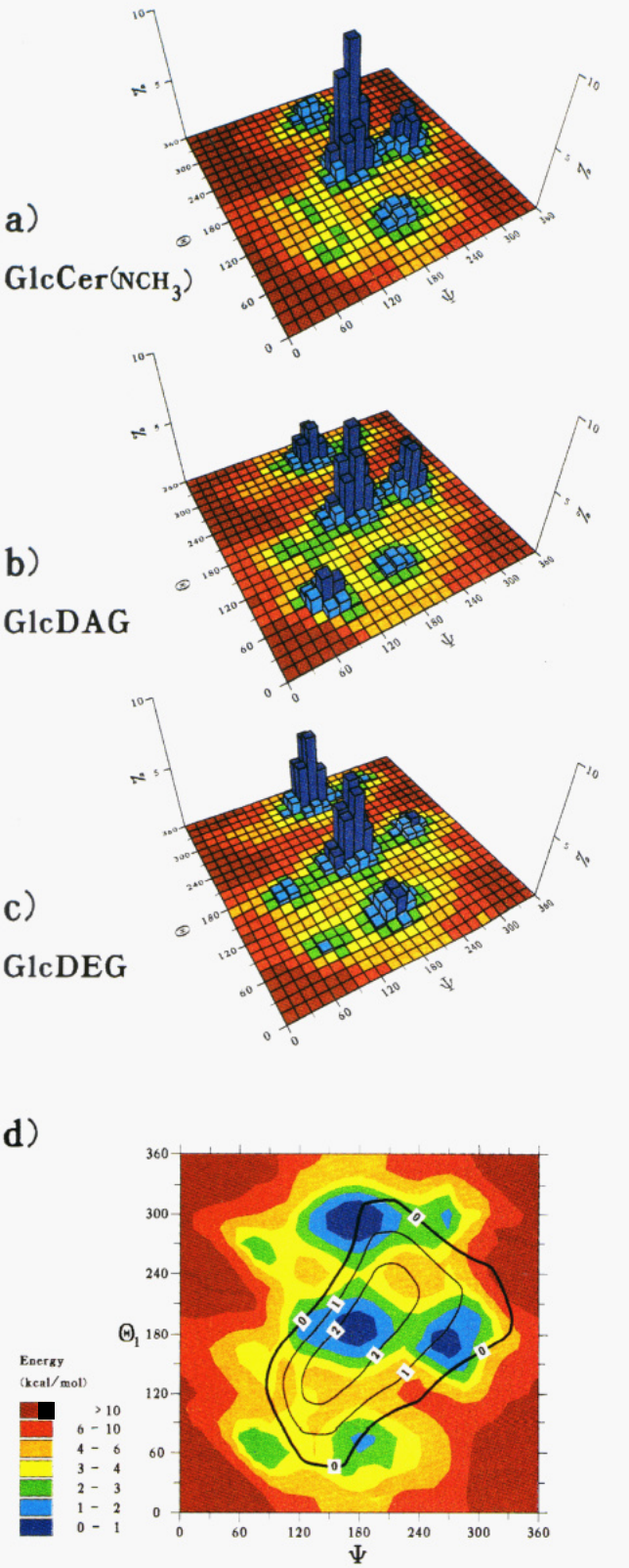

FIGURE 4: (a–c) Combined energy and probability ψ/θ_1 maps for GlcCer(NCH_3) (a), GlcDAG (b), and GlcDEG (c) based on MM3 relaxed map calculations at a dielectric constant of 4. The calculations indicate a preference for conformer 5 (ψ/θ_1 = ap/ap) in all three compounds (for discussion see text). (d) Restrictions due to steric interference of the glucose head group with the membrane surface. The contour lines indicate the minimum distance (in Å) of the headgroup atom of GlcCer(n) from the restriction plane (at the level of C1 in the lipid moiety; cf. Figure 3b) as a function of the torsion angles ψ/θ_1 of the glucose–ceramide linkage. These contours are superimposed on the ψ/θ_1 energy map of GlcCer(n) calculated at $\epsilon = 4$. Note that ψ/θ_1 conformations outside the 0 contour violate the restriction plane.

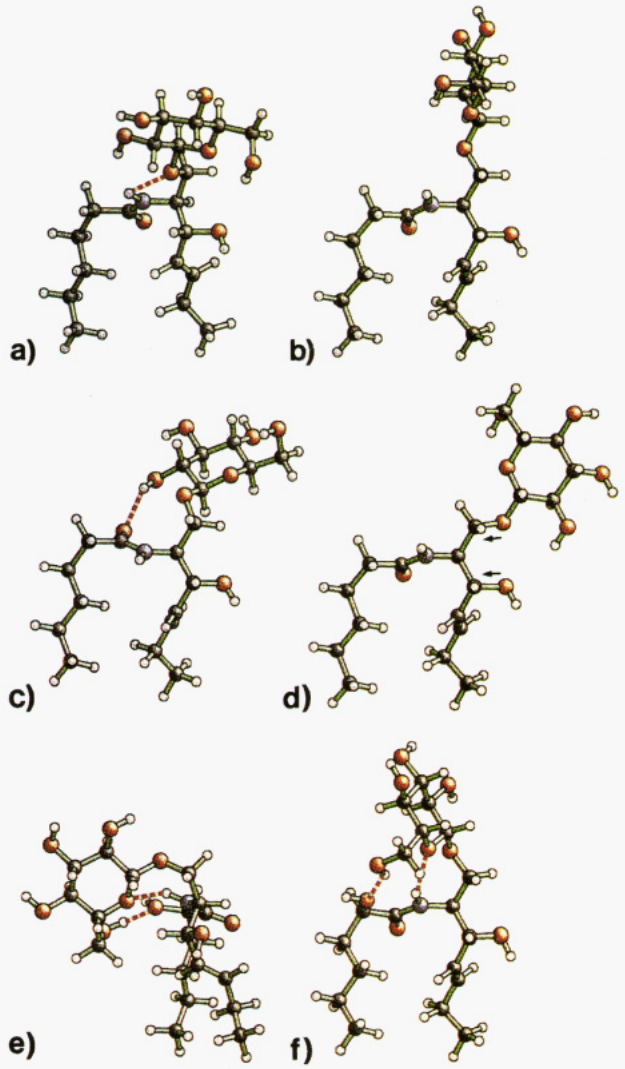

FIGURE 5: Ball-and-stick models of selected minimum energy conformations obtained after complete MM3 minimization. (a) Conformer 2 of GlcCer(n) minimized at $\epsilon = 4$. The hydrogen bond contact between N–H and the sphingosine O1 (N–H···O angle = 100°) is indicated. Note the favorable, antiparallel, arrangement of the N–H and C1–O1 dipoles in the ceramide part. (b) Conformer 5 of GlcCer(n) minimized at $\epsilon = 4$. (c) Conformer 6 of GlcCer(n) minimized at $\epsilon = 4$ showing a stabilizing hydrogen bond between the glucose 2-OH group and the carbonyl oxygen atom. (d) Conformer 8 of GlcCer(n) minimized at $\epsilon = 4$. In sphingolipids the θ_1 = +sc rotamer (in combination with θ_3 = ap) is unfavored due to the 1–3 synaxial orientation of the O1–C1 and O3–C3 bond dipoles (arrows) of the sphingosine moiety. (e) Conformer 1 of GlcCer(h) minimized at $\epsilon = 1.5$. Two hydrogen bonds are indicated: one between the glucose O6 and the 2-OH group of the fatty acid and the other between glucose O5 and the amide hydrogen. Note the back-folding of the head group which makes this conformer unfavorable in a membrane arrangement. (f) Conformer 4 of GlcCer(h) minimized at $\epsilon = 1.5$. Similar to conformer 1 (e), this conformer is stabilized by a hydrogen bond between the 2-OH group on the fatty acid and the 6-OH group on the glucose residue as well as by a hydrogen bond between glucose O5 and the amide hydrogen.

GlcCer(n). This is due to the fact that methylation of the amide nitrogen atom abolishes the NH···O(1) interaction and introduces steric hindrance for the –sc rotamer (conformers 1–3). The major population of the θ_1 rotamers for GlcCer-(NCH_3) is consequently shifted to the ap range and mainly distributed on conformers 5 and 6 (Figure 4a).

ψ/θ_1 Energy Maps of the Glycerolipids GlcDEG and GlcDAG. Calculations of the ψ/θ_1 probability maps of GlcDEG and GlcDAG at $\epsilon = 4$ (Figure 4b,c) show a preference for ψ/θ_1 = ap/ap (conformer 5). In the case of the ester compound GlcDAG there are also significant populations at ψ/θ_1 = ap/–sc (conformer 2), ψ/θ_1 = –sc/ap (conformer 6), and ψ/θ_1 = +sc/+sc (conformer 7) (cf. Table I). Conformer 6 of GlcDAG is stabilized by a hydrogen bond interaction between the glucose 2-hydroxyl group and the carbonyl oxygen of the 2-fatty acid as in the case of glucosylceramides. Conformers 5 and 6 together account for the high population of the ap rotamer of θ_1 (+sc:ap:–sc = 17:63:20%, Table II) for GlcDAG. In conformer 7 of GlcDAG there is a hydrogen bond interaction between the glucose O6 hydroxyl group and the carbonyl oxygen of the γ-fatty acid.

GlcDEG shows a preference for the ap conformation of ψ, and the population is distributed on the staggered conformations of θ_1 in the proportions +sc:ap:–sc = 13:49:37% (Table II).

Conformational Restrictions Imposed by the Membrane Layer. The above described calculations have all been performed on isolated glycolipid molecules. In order to account for the steric restrictions imposed by the surrounding membrane layer, an exclusion plane at the level of C1 of the ceramide was introduced (cf. Figure 3b). These calculations (Figure 4d) indicate that for GlcCer all three staggered rotamers of θ_1 with ψ = ap (conformers 2, 5, and 8) as well as a wide range of ψ at θ_1 = ap (conformers 4, 5, and 6) are allowed. However, the calculations also show that conformational ranges 1, 3, 7, and 9 in the four corners of the ψ/θ_1 map are disfavored for glucosylceramide in a membrane structure since in these conformations the head group would fold back into the membrane layer (cf. Figure 3b).

DISCUSSION

According to the present calculations on glucosylceramides and glucosylglycerides, the torsion angle ϕ of the saccharide–ceramide/diglyceride linkage shows a strict preference for the +sc conformation (Figure 2) irrespective of modifications in the structure of the lipid moiety and variations in the dielectric constant. The torsion angles ψ and θ_1, on the other hand, exhibit a considerable flexibility which for ψ comprises the torsional range from +sc to –sc and for θ_1 preferentially the two staggered conformations –sc and ap (Figure 3, Table II). The features of the ψ/θ_1 maps (Figures 3 and 4), however, were found to be dependent on the structure of the ceramide or diglyceride part and on the choice of the dielectric constant in the calculations. At low ϵ values ($\epsilon = 4$ and $\epsilon = 1.5$) certain ψ/θ_1 conformations are favored due to a stabilization by intramolecular hydrogen bonds and dipole–dipole interactions.

ϵ values that appropriately reflect the dielectric properties within the head-group region of glycolipid-containing bilayers are not available from experimental determinations. However, measurements on phospholipid bilayers indicate a dielectric constant of ϵ = 4–20 for the head-group region (Tocanne & Teissie, 1990), and theoretical calculations suggest a value of 4–10 (Cevc, 1990) at the interface between the hydrocarbon matrix ($\epsilon = 2$) and the head-group region. Since the head groups of glycolipids are apparently less polar and less hydrated (Ruocco & Shipley, 1983) than those of the charged phospholipids, a dielectric constant at the lower end of this ϵ range can be expected at the level of the saccharide–ceramide linkage in bilayers of glycolipids. Therefore, a dielectric constant of $\epsilon = 4$ was used in order to account, within the limitations of an MM3 calculation, for hydrogen bonds and dipole–dipole interactions of a strength relevant for the microenvironment at the interface between the head-group region and the hydrocarbon matrix. The necessity to account for these interactions is highly emphasized by the known effects

of hydrogen bonding on the structural properties of glycosphingolipids (Boggs, 1987; Curatalo, 1987). In this respect calculations with MM3 are more appropriate than calculations with the HSEA method (Lemieux et al., 1980; Thøgersen et al., 1982) in which the polar interactions are neglected.

Preferred Conformations of Glucosylceramides. The strict preference of ϕ for the +sc range is in accordance with the crystal structures of galactosylceramide (Pascher & Sundell, 1977), permethylated galactosylceramide (Nyholm et al., 1990), glucosylphytosphingosine (Abrahamsson et al., 1977), and numerous other crystal structures of β-glycosides (Jeffrey & Taylor, 1980). The ϕ = +sc conformation is also confirmed by NMR studies and is fully in line with the concept of the exo-anomeric effect (Lemieux et al., 1979; Lemieux, 1984).

With respect to the ψ/θ_1 energy surface the glycosylceramides generally show a preference for –sc and ap rotamers of θ_1, whereas the +sc rotamer is disfavored (Figure 3c–g, Table II). The high relative energy for the +sc conformation of θ_1 can be explained by a Hassel–Ottar effect [cf. Hassel and Ottar (1947)] which arises in this rotamer due to a 1,3-synaxial orientation of the sphingosine C1–O1 and C3–O3 bonds (Figure 3b, conformers 7–9, and Figure 5d). The Hassel–Ottar effect (HO effect), which is considered to be due to the parallel arrangement of C–O dipoles (Jeffrey, 1990), has earlier been described in the case of the C5–C6 bond of 1–6 glycosidic linkages (Marchessault & Perez, 1979; Brisson & Carver, 1983; Cummming & Carver, 1987; Wooten et al., 1990) and been estimated to 3 kcal/mol (Marchessault & Perez, 1979). In sphingolipids the HO effect should quite generally suppress the +sc rotamer of θ_1. Moreover the HO effect in conjunction with the energy barrier of the eclipsed sp range of θ_1 restricts the possible rotation of the C1–C2 bond and should thus affect the dynamics of the saccharide head group in GSLs.

Within the low-energy regions of the ψ/θ_1 map at θ_1 = –sc and ap (Figure 3, regions 2–3 and 5–6), the positions of the energy minima are to a large extent determined by intramolecular dipole–dipole interactions and hydrogen bonds as is obvious from calculations at different values of the dielectric constant (Figure 3c–g). Calculations carried out at ϵ = 4 (Figure 3d,f) show a strong preference for three distinct regions of the ψ/θ_1 map corresponding to conformers 2, 5, and 6 (Figure 5a–c) which together account for >85% of the total population.

Conformer 2 (ψ/θ_1 = ap/–sc), which is dominating in the ψ/θ_1 probability map (almost 50% of the population), represents the global energy minimum (ψ/θ_1 = 178°/–63°, Table I), of GlcCer(n) and GlcCer(h) at ϵ = 4. This conformation is stabilized by dipole–dipole interactions between the N–H and C1–O1 dipoles as well as by a weak hydrogen bond between H(N) and O1 (Figure 5a). The torsion angles ψ/θ_1 of conformer 2 are in agreement with the conformation of the galactose–ceramide linkage in the crystal structure of cerebroside (Pascher & Sundell, 1977). This comparison between GlcCer and the corresponding galactosylceramide is justified as the only structural difference—the chirality at C4 of the sugar residue—has no significant effects on the energetics of the saccharide–ceramide linkage (Nyholm, unpublished results).

The preference for the –sc rotamer of θ_1 is also in agreement with *J*-coupling NMR data on sphingomyelin (Bruzik, 1988) and cerebroside (Bruzik, personal communication). Furthermore, the preference for conformer 2 is in agreement with earlier minimum energy calculations on GlcCer(h) (Wynn, 1986) and with MM2 calculations on galactosylceramide (Nyholm et al., 1990).

In conformer 6 (ψ/θ_1 = –sc/ap; see Table I) there is a stabilizing hydrogen bond between the glucose 2-OH group and the amide carbonyl oxygen (Figure 5c). This ψ/θ_1 conformation has been observed in the crystal structure of permethylated cerebroside (Nyholm et al., 1990) despite of the fact that the indicated hydrogen bond is abolished by methylation.

In the case of conformer 5 (ψ/θ_1 = ap/ap), which is favored by its all-antiplanar conformation, there is so far no corresponding crystal structure. However, the existence of a conformer with extended head group is indicated by NMR results obtained for glucosylceramide in multilamellar systems (Skarjune & Oldfield, 1982).

A comparison of the ψ/θ_1 maps of GlcCer(n) and GlcCer(h) indicates a close similarity both at ϵ = 80 and at ϵ = 4 (Figure 3). However, in calculations at ϵ = 1.5 (Figure 3e,g) there are drastic differences between GlcCer(n) and GlcCer(h). For GlcCer(h) conformers 1 and 4 are stabilized by hydrogen bond interactions involving the 2-OH group of the fatty acid (Figure 5e,f) whereas for GlcCer(n) conformer 6 (Figure 5c) becomes completely dominating. However, when the geometries obtained at ϵ = 1.5 are used as starting geometries for a recalculation of the ψ/θ_1 energy map at ϵ = 4, the dominating influence of these interactions does not persist. The pronounced differences in conformational preferences at ϵ = 1.5 and 4 can be explained by the fact that the strength of hydrogen bonds is enhanced as a direct consequence of the low ϵ value and additionally due to a more efficient optimization of the hydrogen bond geometry.

Apparently conformers 1 and 4 of GlcCer(h) are critically dependent on strong hydrogen bond interactions (in vacuo conditions). Thus, although these calculations at ϵ = 1.5 suggest a possibility for conformational differences between GlcCer(n) and GlcCer(h), the relevance of these results for bilayer conditions remains unclear. This issue will be a target for further studies.

Preferred Conformations of Glucosylglycerolipids. In the case of the glucosylglycerolipids, GlcDAG and GlcDEG, MM3 calculations at ϵ = 4 indicate a preference for the ap conformation of θ_1, in particular, conformer 5 (Figure 4b,c, Tables I and II). The difference between glucosylceramides and glucosylglycerolipids with respect to preferences for θ_1 rotamers is due to the fact that the amide N–H group, which in GSLs stabilizes the θ_1 = –sc conformation, is lacking in glycoglycerolipids.

Furthermore, in glycerolipids the lack of a HO effect results in a somewhat higher population of the +sc rotamer (Figure 4b,c Tables I and II) than in the case of glucosylceramides. However, the population of the +sc rotamer of θ_1 is still lower than that of the ap and –sc rotamers. This appears to be due to the fact that the ap and –sc rotamers but not the +sc rotamer of θ_1 are stabilized by a gauche effect (Abe & Mark, 1976) which favors the ±sc conformation for the atom sequence O1–C1–C2–O2 of the glycerol moiety (Pascher et al., 1992).

Conformer 5 (ψ/θ_1 = ap/ap), which according to the MM3 calculations is the dominating conformer for the glucosylglycerolipids, is compatible with the "extended" model for GlcDEG as derived from NMR data of multilamellar systems (Jarrell, 1987; Renou et al., 1989).

The differences in calculated conformational preferences between glycosylceramides and the corresponding glycerolipids suggest a possible explanation to the differences in reactivity with galactose oxidase (Lingwood, 1976) and differences in phase behavior (Curatalo, 1987; Boggs, 1987) observed for these two groups of lipids. It may be inferred that the preferred

extended conformation of the saccharide head group in glycoglycerolipids (cf. Figure 5b) allows a close head-group packing which in lipid–water systems favors the formation of a hexagonal (H_{II}) phase (Boggs, 1987). On the other hand, the larger packing cross section of the more layer-parallel head group in sphingolipids (conformer 2, Figure 5a) rather favors the formation of lamellar structures (Ruocco et al., 1981).

Restrictions Imposed by the Membrane Layer. In order to predict favored orientations of the saccharide head group for glycolipids arranged in a membrane layer, it is necessary to account also for restrictions imposed by the surrounding lipid layer (Nyholm et al., 1989). These restrictions are basically related to steric hindrance and the dehydration involved in the translocation of the polar saccharide group into the bilayer phase. Since the energy profile for the penetration of a polar residue into bilayers is poorly explored, the present analysis was confined to a mere calculation of distances of the saccharide head-group atoms in relation to a theoretical plane corresponding to the interface between the core and head-group region of the lipid bilayer (Figure 3b). The calculations show that for the studied monoglucosylipids several conformations of the ψ/θ_1 map (e.g., conformers 1, 3, 7, and 9, Figure 4d) are excluded due to interference of the glucose residue with the membrane layer. This causes a considerable reduction of the conformational space available for the glucose head group.

Extensions of the saccharide head group with further sugar residues do not significantly affect the intrinsic conformational preferences of the saccharide–ceramide linkage (Nyholm, unpublished results). However, extensions of the saccharide chain give rise to increased interference with the bilayer surface and further restrict the available range of ψ/θ_1 (Nyholm et al., 1989). Recent studies on the bent and bulky saccharide chains of GSLs of the globo series suggest that conformational restrictions imposed by the surrounding layer are of importance in defining the orientation of the saccharide head group and the accessibility of saccharide epitopes at the membrane surface (Nyholm et al., 1989; Strömberg et al., 1991). These steric restrictions can account for crypticity phenomena observed for the Galα1–4Gal epitope of globoGSLs in natural membranes.

The present study shows that for glycolipids the orientation of the saccharide head group at the membrane surface is determined by an interplay between the intrinsic preferences of the saccharide–ceramide linkage and restrictions due to the surrounding lipid bilayer. Further work is necessary to analyze the significance of the discontinuous polarity of the glycolipid environment at the membrane surface. Such studies will be performed using molecular dynamics simulations (van Gunsteren & Berendsen, 1990) which explicitly account for interactions with surrounding lipid and water molecules.

REFERENCES

Abe, A., & Mark, J. E. (1976) *J. Am. Chem. Soc. 98*, 6468–6476.

Abrahamsson, S., Dahlen, B., & Pascher, I. (1977) *Acta Crystallogr. B33*, 2008–2013.

Allinger, N. L. (1977) *J. Am. Chem. Soc. 99*, 8127–8134.

Allinger, N. L., Yuh, Y. H., & Lii, J.-H. (1989) *J. Am. Chem. Soc. 111*, 8551–8566.

Allinger, N. L., Rahman, M., & Lii, J. H. (1990) *J. Am. Chem Soc. 112*, 8293–8307.

Boggs, J. M. (1987) *Biochim. Biophys. Acta 906*, 353–404.

Brisson, J. R., & Carver, J. P. (1983) *Biochemistry 22*, 3680–3686.

Bruzik, K. S. (1988) *Biochim. Biophys. Acta 939*, 315–326.

Cevc, G. (1990) *Biochim. Biophys. Acta 1031*, 311–382.

Chu, S. S. C., & Jeffrey, G. A. (1968) *Acta Crystallogr. B24*, 830–838.

Cumming, D. A., & Carver, J. P. (1987) *Biochemistry 26*, 6664–6676.

Curatalo, W. (1987) *Biochim. Biophys. Acta 906*, 111–136.

Dewar, M. J., S., Zoebisch, E. G., Healy, E. F., & Stewart, J. J. P. (1985) *J. Am. Chem. Soc. 107*, 3902–3909.

Dowd, M. K., Reilly, P. J., & French, A. D. (1992) *J. Comput. Chem. 13*, 102–114.

French, A. D. (1988) *Biopolymers 27*, 1519–1525.

French, A. D., Rowland, R. S., & Allinger, N. L. (1990a) in *Computer Modeling of Carbohydrate Molecules*, ACS Symposium Series, No. 430, pp 120–140, American Chemical Society, Washington, DC.

French, A. D., Tran, V. H., & Perez, S. (1990b) in *Computer Modeling of Carbohydrate Molecules*, ACS Symposium Series, No. 430, pp 191–212, American Chemical Society, Washington, DC.

Ha, S. N., Madsen, L. J. & Brady, J. W. (1988) *Biopolymers 27*, 1927–1952.

Hakomori, S.-i. (1989) *Adv. Cancer Res. 52*, 257–331.

Hakomori, S.-i. (1990) *J. Biol. Chem. 265*, 18713–18716.

Hassel, O., & Ottar, B. (1947) *Acta Chem. Scand. 1*, 929–943.

Hauser, H., Pascher, I., Pearson, R. H., & Sundell, S. (1981) *Biochim. Biophys. Acta 650*, 21–51.

Jarrell, H. C., Giziewicz, J. B., & Smith, I. C. P. (1986) *Biochemistry 25*, 3950–3957.

Jarrell, H. C., Jovall, P. Å., Giziewicz, J. B., Turner, L. A., & Smith, I. C. P. (1987) *Biochemistry 26*, 1805–1811.

Jeffrey, G. A. (1990) *Acta Crystallogr. B46*, 89–103.

Jeffrey, G. A., & Taylor, R. (1980) *J. Comput. Chem. 1*, 99–109.

Kanfer, J. N., & Hakomori, S.-i. (1983) *Handbook of Lipid Research. Sphingolipid Biochemistry*, Plenum Press, New York.

Karlsson, K. A. (1989) *Annu. Rev. Biochem. 58*, 309–350.

Klyne, W., & Prelog, V. (1960) *Experientia 16*, 521–523.

Lemieux, R. U. (1985) in *Proceedings of the VIIIth International Symposium on Medicinal Chemistry* (Dahlbom, R., & Nilsson, J. L. G., Eds.) Vol. 2, pp 329–351, Swedish Pharmaceutical Press, Stockholm.

Lemieux, R. U., Koto, S., & Voisin, D. (1979) in *The anomeric effect: Origin and consequences* (Szarek, W. A., & Horton, D., Eds.) ACS Symposium Series, No. 87, pp 17–29, American Chemical Society, Washington, DC.

Lemieux, R. U., Bock, K., Delbaere, T. J., Koto, S., & Rao, V. S. (1980) *Can. J. Chem. 58*, 631–653.

Lii, J. H., & Allinger, N. L. (1991) *J. Comput. Chem. 12*, 186–199.

Lii, J. H., Gallion, S., Bender, C., Wikström, H., Allinger, N. L., Flurchick, K. M., & Teeter, M. M. (1989) *J. Comput. Chem. 10*, 503–513.

Lingwood, C. A. (1979) *Can. J. Biochem. 57*, 1138–1143.

Marchessault, R. H., & Perez, S. (1979) *Biopolymers 18*, 2369–2374.

Norskov-Lauritsen, L., & Allinger, N. L. (1984) *J. Comput. Chem. 5*, 326–335.

Nyholm, P. G., Breimer, M., Samuelsson, B. E., & Pascher, I. (1989) *J. Mol. Recogn. 2*, 103–113.

Nyholm, P. G., Pascher, I., & Sundell, S. (1990) *Chem. Phys. Lipids 52*, 1–10.

Pascher, I., & Sundell, S. (1977) *Chem. Phys. Lipids 20*, 175–191.

Pascher, I., Lundmark, M., Nyholm, P. G., & Sundell, S. (1992) *Biochim. Biophys. Acta 1113*, 339–373.

Paulsen, H., Peters, T., Sinnwell, V., Lebuhn, R., & Meyer, B. (1984) *Liebigs Ann. Chem.*, 951–976.

Poppe, L., von der Lieth, C. W., & Dabrowski, J. (1990) *J. Am. Chem. Soc. 112*, 7762–7771.
Renou, J. P., Giziewicz, J. B., Smith, I. C. P., & Jarrell, H. C. (1989) *Biochemistry 28*, 1804–1814.
Ruocco, M. J., & Shipley, G. G. (1983) *Biochim. Biophys. Acta 735*, 305–308.
Ruocco, M. J., Atkinson, D., Small, D. M., Skarjune, R. P., Oldfield, E., & Shipley, G. G. (1981) *Biochemistry 20*, 5957–5966.
Skarjune, R., & Oldfield, E. (1982) *Biochemistry 21*, 3154–3160.
Stewart, J. J. P. (1990) *J. Comput.-Aided Mol. Design 4*, 1–105.
Strömberg, N., Nyholm, P. G., Pascher, I., & Normark, S. (1991) *Proc. Natl. Acad. Sci. U.S.A. 88*, 9340–9344.
Thøgersen, H., Lemieux, R. U., Bock, K., & Meyer, B. (1982) *Can. J. Chem. 60*, 44–57.
Tocanne, J. F., & Teissie, J. (1990) *Biochim. Biophys. Acta 1031*, 111–142.
van Gunsteren, W. F., & Berendsen, H. J. C. (1990) *Angew. Chem., Int. Ed. Engl. 29*, 992–1023.
Wooten, E. W., Bazzo, R., Edge, C. J., Zamze, S., Dwek, R. A., & Rademacher, T. W. (1990) *Eur. Biophys. J.*, 139–148.
Wynn, C. H., Marsden, A., & Robson, B. (1986) *J. Theor. Biol. 119*, 81–87.